jmb Article

Exploring the Basis of [*PIN*$^+$] Variant Differences in [*PSI*$^+$] Induction

Jaya Sharma[1] and Susan W. Liebman[1,2]

*1 - **Department of Biological Sciences,** University of Illinois at Chicago, Chicago, IL 60607, USA*
*2 - **Department of Biochemistry and Molecular Biology,** University of Nevada, Reno, NV 89557, USA*

***Correspondence to Susan W. Liebman:** Department of Biochemistry and Molecular Biology, University of Nevada, 1664 North Virginia Street, Reno, NV 89557, USA. sueL@uic.edu*
http://dx.doi.org/10.1016/j.jmb.2013.06.006
Edited by R. Wetzel

Abstract

Certain soluble proteins can form amyloid-like prion aggregates. Indeed, the same protein can make different types of aggregates, called variants. Each variant is heritable because it attracts soluble homologous protein to join its aggregate, which is then broken into seeds (propagons) and transmitted to daughter cells. [*PSI*$^+$] and [*PIN*$^+$] are respectively prion forms of Sup35 and Rnq1. Curiously, [*PIN*$^+$] enhances the *de novo* induction of [*PSI*$^+$]. Different [*PIN*$^+$] variants do this to dramatically different extents. Here, we investigate the mechanism underlying this effect. Consistent with a heterologous prion cross-seeding model, different [*PIN*$^+$] variants preferentially promoted the appearance of different variants of [*PSI*$^+$]. However, we did not detect this specificity *in vitro*. Also, [*PIN*$^+$] variant cross-seeding efficiencies were not proportional to the level of Rnq1 coimmunocaptured with Sup35 or to the number of [*PIN*$^+$] propagons characteristic for that variant. This leads us to propose that [*PIN*$^+$] variants differ in the cross-seeding quality of their seeds, following the Sup35/[*PIN*$^+$] binding step.
© 2013 Elsevier Ltd. All rights reserved.

Introduction

Prions are infectious protein aggregates capable of self-propagation. In mammals, the normal cellular PrP^C (prion protein), which is α-helical, can fold in a β-sheet-rich amyloid form called PrP^{Sc}, which causes fatal neurodegenerative diseases [1]. PrP^{Sc} is infectious because it converts PrP^C into PrP^{Sc} in an autocatalytic fashion [2]. Curiously, there are different heritable forms of PrP^{Sc}, called strains, which cause neurodegenerative diseases with different characteristics and pathologies [3–5]. How these distinct prion strains are generated and how they cause distinct pathologies is unknown.

Amyloid diseases are also associated with the conversion of normally folded protein into amyloid that is deposited in various tissues. For example, Alzheimer's disease is associated with Aβ (amyloid beta-protein) amyloid, Huntington's disease is associated with mutant huntingtin amyloid, Parkinson's disease is associated with α-synuclein amyloid, and type II diabetes is associated with insulin amyloid precursor peptide [6].

Prions also occur in yeast and fungi where they confer specific heritable phenotypes that are transmitted in a dominant non-Mendelian fashion [7–13]. Analogous to the mammalian PrP strains, individual yeast prion proteins can fold in multiple heritable conformations that cause distinct differences in the degree of the altered phenotypes they cause [14–18].

For both the yeast and PrP proteins, a subregion, called the prion domain, is required for prion maintenance and propagation [14,19–21]. Most known yeast prion domains, but not PrP, are rich in glutamines (Q) and/or asparagines (N) [8,9,12,22,23]. Although there is no sequence similarity or functional resemblance between the yeast prions and the mammalian PrP^{Sc} prion, they share the properties of being in β-sheet-rich, amyloid-like, and protease-resistant aggregates [24–26].

Once a protein forms an amyloid "seed", soluble molecules of the same protein join the amyloid fiber ends and are converted into the seed's conformation. For a prion to be inherited in yeast, a variety of chaperones, including Hsp104 and Sis1, are required to shear the amyloid aggregate [27–30]. This

creates more ends available to bind and convert soluble protein and cuts the aggregate into pieces that can be transmitted to daughter cells [31]. Indeed, deletion of Hsp104 eliminates the propagation of most known yeast prions [7–9,13,32–34], as does growth in the presence of low levels of guanidine hydrochloride (GuHCl) that inactivates Hsp104 [35,36].

Two of the best studied yeast prions [*PSI*$^+$] and [*PIN*$^+$] (also called [*RNQ*$^+$]) are respectively the prion forms of the Sup35 and Rnq1 proteins [7,13,32,37]. Sup35 is a translation termination factor, while the function of Rnq1 is unknown [38]. The prion domain of Rnq1 is Q/N rich and is located in the C-terminal region of the protein (amino acids 132–405) [13,39,40]. Sup35 is composed of three structural domains: the Q/N-rich N-terminal (amino acids 1–123) domain, the middle M-domain (amino acids 124–254), and the C-domain (amino acids 255–685) [14,21,41]. The Sup35N-domain functions in RNA turnover [42] and is necessary and sufficient for prion formation and aggregation [14,43]. The Sup35M-domain is not essential for prion formation or translation termination but affects the phenotypes and maintenance of [*PSI*$^+$] variants [41,44]. The Sup35C-domain is essential for translation termination and, thus, for cell viability [21]. When in the prion form, Sup35 has reduced translation termination factor activity and this causes some read through of nonsense mutations [10,11,45].

Different heritable variants of [*PSI*$^+$] were originally distinguished on the basis of their efficiency of nonsense suppression. This is conveniently assayed using the *ade1-14* nonsense mutation, which causes normally white yeast to become red in the absence of suppression. The color can be restored to white in proportion to the level of read through of the *ade1-14* premature nonsense codon [33,46]. In *ade1-14* cells, variants called strong [*PSI*$^+$] were white in color because they caused efficient aggregation of Sup35 and thus efficient nonsense suppression. Variants called weak [*PSI*$^+$] were pink in color because they had less efficient aggregation of Sup35 and thus nonsense suppression. Also, weak [*PSI*$^+$] showed reduced mitotic stability relative to strong [*PSI*$^+$], in the presence [47] and absence [14,32,48] of [*PIN*$^+$]. Although [*PSI*$^+$] variants are generally categorized as strong or weak, there is a continuum of variants with different levels of nonsense suppression varying from very weak to very strong [*PSI*$^+$] [49].

[*PSI*$^+$] variants differ in the size of SDS-resistant Sup35 polymers. Stronger variants contain smaller polymers than weaker variants [27], presumably because they are more susceptible to fragmentation by Hsp104 [17,50]. Since variants with smaller Sup35 polymer contain more fiber ends, they more efficiently recruit soluble Sup35, resulting in reduced amounts of functional Sup35.

The examination of other criteria, such as responses to chaperones and efficiency of transmission of [*PSI*$^+$] to [*psi*$^-$] cells with certain Sup35 mutations or to cells with Sup35 encoded by other species, [17,51–55] has recently shown that [*PSI*$^+$] variants with the same color are not necessarily identical [56,57]. Nonetheless, the color assay continues to allow a simple distinction between different types of [*PSI*$^+$] variants.

Overexpression of the prion domain of Sup35 induces *de novo* [*PSI*$^+$] formation presumably because the increased concentration of the Sup35 prion domain makes it more likely that some of the domain molecules will misfold and seed continued conversion. The frequency of this induction of [*PSI*$^+$] is dramatically increased by the presence of another prion, for example, [*PIN*$^+$] [32]. However, once [*PSI*$^+$] is established, [*PIN*$^+$] can be lost and [*PSI*$^+$] continues to propagate [58].

One idea to explain how [*PIN*$^+$] enhances the appearance of [*PSI*$^+$] is that the [*PIN*$^+$] prion binds to and inactivates cellular factors that would otherwise inhibit *de novo* [*PSI*$^+$] prion formation [59]. Currently, there is no evidence to support this hypothesis. Rather, several lines of evidence support a heterologous cross-seeding mechanism in which the [*PIN*$^+$] prion enhances the appearance of [*PSI*$^+$] by providing an inefficient template for the conversion of soluble Sup35 monomers into amyloid [7].

The heterologous cross-seeding hypothesis is supported by the findings that the efficiency of *in vitro* Sup35NM polymerization into amyloid is enhanced by the addition of heterologous amyloid fiber, for example, Rnq1 as well as other QN-rich but also some non-QN-rich fibers [60,61]. Furthermore, in such experiments, the newly appearing Sup35NM fibers were seen by electron microscopy to emerge from globular aggregates of the Rnq1 prion domain [60]. Also, newly appearing [*PSI*$^+$] aggregates induced and visualized *in vivo* with overexpressed Sup35NM-YFP always overlapped with [*PIN*$^+$] aggregates visualized with overexpressed Rnq1-CFP. However, this result is complicated by the fact that the overexpression of Rnq1-CFP increases the size and reduces the number of [*PIN*$^+$] aggregates. Indeed, even in cells with established [*PSI*$^+$], there was often, although not always, overlap between the overexpressed Sup35NM-YFP and Rnq1-CFP aggregates [61]. In contrast, in cells with no overexpression, established [*PSI*$^+$] and [*PIN*$^+$] prions appear to form separate structures lacking a tight interaction [62]. However, even without overexpression of Rnq1, large Sup35 aggregates that appear when Sup35 is overexpressed in [*PIN*$^+$][*psi*$^-$] cells copurified with Rnq1 [63]. These large aggregates are in the shape of rings or lines [64,65] and appear prior to the appearance of *bona fide* [*PSI*$^+$] [63].

Other support for the cross-seeding model is that [*PSI*$^+$] appears rapidly *de novo* in [*PIN*$^+$] cells

expressing low levels of a fusion of the Rnq1 and Sup35 prion domains [66]. Since the Rnq1 domain of the fusion efficiently joins the [*PIN*$^+$] aggregate, it also efficiently brings the fused Sup35 prion domain to the vicinity of the [*PIN*$^+$] aggregate, which was proposed to promote heterologous cross-seeding. In addition, several mutations in the prion domain of Rnq1 can maintain the [*PIN*$^+$] prion but reduce its ability to promote the induction of [*PSI*$^+$]. This suggests a direct Rnq1/Sup35 interaction through the mutated sites [67].

Heterologous cross-seeding of amyloids also appears to be a risk factor for human diseases. Mice injected with amyloid-like fibrils made of a variety of peptides promoted the formation of amyloid protein A, which is associated with systemic AA amyloidosis [68]. Heterologous cross-seeding has also been observed between the Alzheimer-associated Aβ peptide and the islet amyloid polypeptide [69], and between Aβ and PrP [70]. Also, Aβ fibers appear to induce the amyloidosis of tau [71,72].

Like PrP and [*PSI*$^+$], the [*PIN*$^+$] prion exists in different heritable forms. These [*PIN*$^+$] variants have been distinguished on the basis of their ability to cause overexpressed SUP35NM-GFP to form fluorescent rings [64], which reflects their ability to induce [*PSI*$^+$], and the relative amount of aggregated *versus* soluble Rnq1 protein present. High [*PIN*$^+$] forms rings and induces [*PSI*$^+$] with the highest frequency and contains the least soluble Rnq1, whereas low [*PIN*$^+$] forms rings and induces [*PSI*$^+$] with the lowest efficiency and contains more soluble Rnq1. However, surprisingly very high [*PIN*$^+$], the variant with the highest efficiency of ring and [*PSI*$^+$] induction, contains the most soluble Rnq1 [15]. Some [*PIN*$^+$] variants can also be distinguished by the microscopic appearance of fluorescent aggregates caused by overexpressing Rnq1-GFP. Such aggregates appear as a single dot per cell in the presence of low or very high [*PIN*$^+$] and as multiple dots per cell in the presence of high [*PIN*$^+$]. It is important to recall that these visible RNQ1-GFP aggregates are not the infectious prion seeds but are just a variant-specific characteristic of the prion in the presence of overexpressed RNQ1-GFP.

Here, we investigated the effects of [*PIN*$^+$] variant differences on the induction of [*PSI*$^+$]. In support of the heterologous cross-seeding model, different [*PIN*$^+$] variants preferentially promoted the *in vivo* appearance of specific variants of [*PSI*$^+$]. However, there was no specificity *in vitro*, suggesting the critical involvement of cellular factors. Also, [*PIN*$^+$] variants did not differ in their ability to bind to Sup35, nor did differences in their propagon numbers reflect their different phenotypes. Rather, it appears that the [*PIN*$^+$] variants differ in the cross-seeding quality of their seeds.

Results

Specific [*PIN*$^+$] variants preferentially seed specific [*PSI*$^+$] variants *in vivo*

The cross-seeding model predicts that [*PIN*$^+$] aggregates act as an inefficient template to cross-seed *de novo* Sup35 aggregation during the initial stages of [*PSI*$^+$] formation. We hypothesized that during this process, the pre-existing [*PIN*$^+$] prion seeds might transfer some of their variant-specific structure to the heterologous [*PSI*$^+$] prion being cross-seeded. This could cause certain [*PIN*$^+$] variants to seed one [*PSI*$^+$] variant more frequently than another, and this preference might be reversed for a different [*PIN*$^+$] variant.

To test this, we asked if specific [*PIN*$^+$] variants preferentially cross-seed specific [*PSI*$^+$] variants. The plan was to induce [*PSI*$^+$] *de novo* by overexpressing Sup35 in the presence of different [*PIN*$^+$] variants. However, since overexpression of Sup35 in the presence of strong [*PSI*$^+$] causes severe toxicity and growth inhibition with less dramatic effects in the presence of weak [*PSI*$^+$] [73], we were concerned that there would be a bias against strong [*PSI*$^+$] isolates. The toxicity arises because [*PSI*$^+$] aggregates bind to and sequester an essential protein [73]. This can be prevented by overexpressing Sup35C, which lacks the prion domain and therefore does not join the prion aggregate, but binds to the essential protein and retains full function in translation. Thus, in our experiments, we overexpressed Sup35C during the induction of [*PSI*$^+$].

Integrated *GAL*::*SUP35* and plasmid-borne *GAL*::*SUP35C* were induced simultaneously in cells bearing

Fig. 1. [*PIN*$^+$] variants differ in their preference for cross-seeding weak *versus* strong [*PSI*$^+$]. (a) Appearance of newly induced [*PSI*$^+$] colonies in the presence of low, high, and very high [*PIN*$^+$]. All cells had an integrated copy of *GAL*::*SUP35* and a plasmid encoding *GAL*::*SUP35C*. Shown are cells plated on YPD following induction of both *SUP35* and *SUP35C* after 4 days of growth on galactose. (b) Determination of the variant type of the sectored colonies. The 600 sectored colonies were each subcloned. Six examples are shown. Those giving rise to only red and white colonies were scored as strong [*PSI*$^+$]. Those giving rise to only red and pink colonies were scored as weak [*PSI*$^+$]. Those giving rise to red, white, and pink colonies were scored as mixed. (c) Frequencies of strong and weak [*PSI*$^+$] isolated in the different [*PIN*$^+$] variants. Shown is the percent of colonies that were not red obtained from low [*PIN*$^+$] (n = 400), high [*PIN*$^+$] (n = 604), and very high [*PIN*$^+$] (n = 1592). Statistical differences ($p < 0.0001$) were seen between the distributions of weak and strong [*PSI*$^+$] obtained from low and high [*PIN*$^+$], from low and very high [*PIN*$^+$], and from high and very high [*PIN*$^+$]. Error bars show the standard error of the mean calculated from more than three independent experiments. A two-by-two contingency table and Fisher's exact two-tailed test were used to calculate p values.

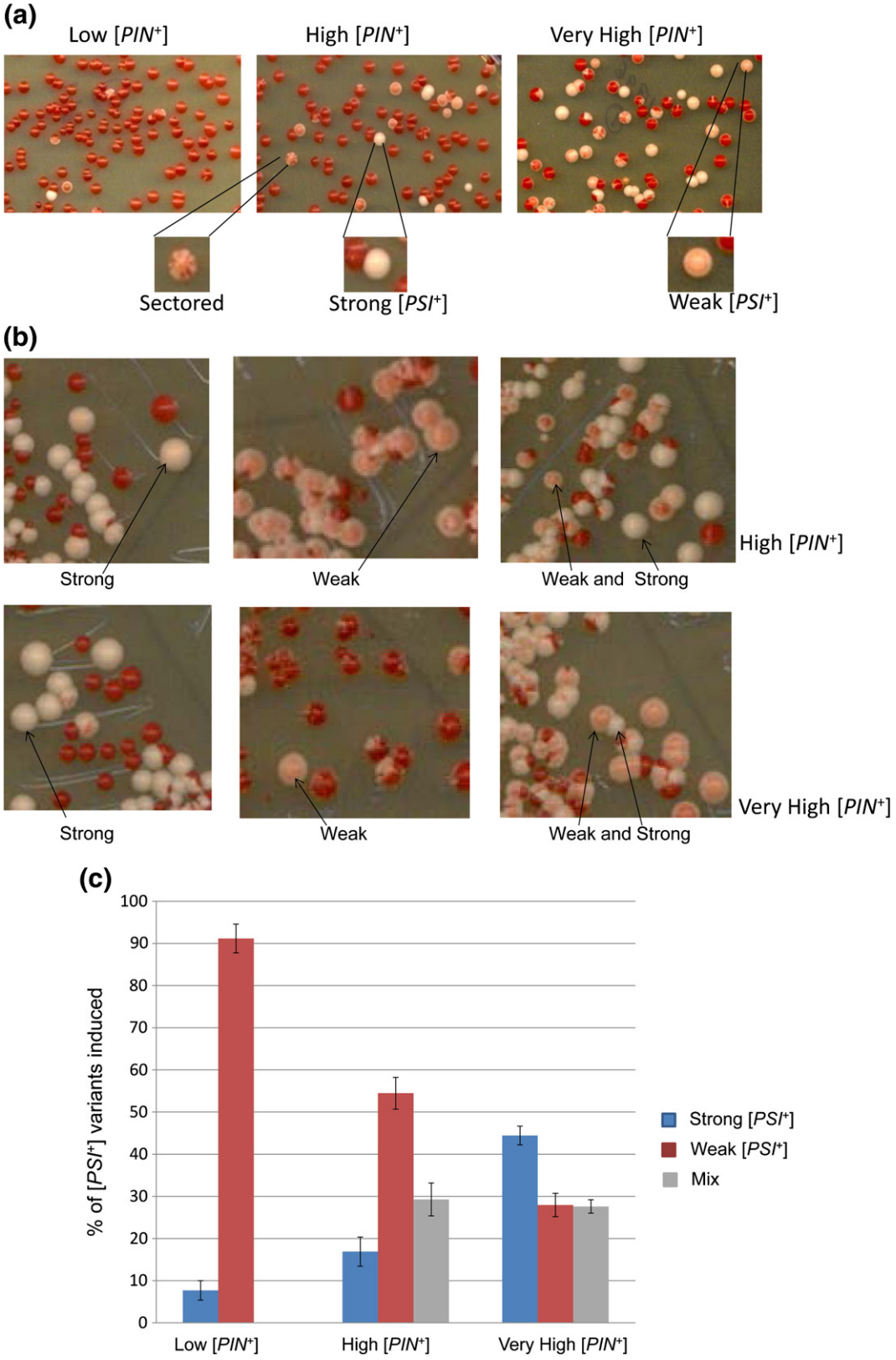


Fig. 1 (*legend on previous page*)

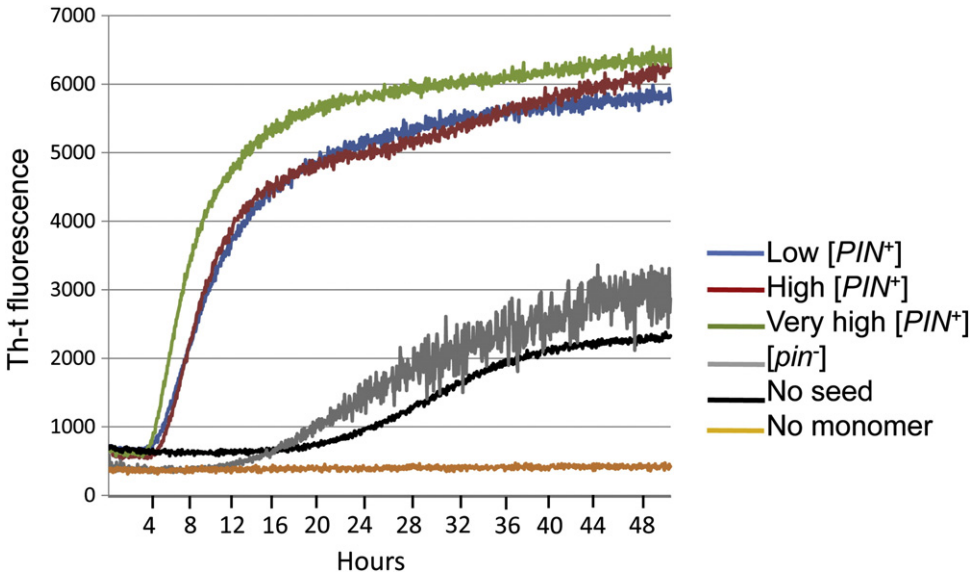


Fig. 2. Purified lysate from [*PIN*$^+$] variants seed [*PIN*$^+$] fibers *in vitro*. Kinetics of polymerization of 40 μM recombinant Rnq1 PD (132–405) agitated 3 min every 10 s for 48 h in the presence of sonicated [*PIN*$^+$] aggregates purified from low, high, and very high [*PIN*$^+$] cells is shown. The rate of amyloid formation was measured by thioflavin T dye binding, which caused fluorescence. Reactions with no aggregate added (no seed) and with the "aggregates" purified from [*pin*$^-$] cells ([*pin*$^-$]) were run as controls.

low, high, or very high [*PIN*$^+$] variants. Cells were then plated and grown on YPD (yeast extract, peptone, dextrose) where colony color was used to distinguish strong [*PSI*$^+$] (white), weak [*PSI*$^+$] (pink), and [*psi*$^-$] (red). As noted previously, newly induced [*PSI*$^+$] is often unstable, so many of the lighter color colonies had numerous red [*psi*$^-$] sectors [47,49,74] (Fig. 1a). The frequencies of appearance of all non-red colonies including pink, white, and sectored colonies were determined. Non-red colonies were tested for their [*PSI*$^+$] status using the Sup35NM-GFP aggregate decoration assay by crossing them with a [*psi*$^-$] strain carrying p*Cup1-SUP35NM-GFP*. More than 98% showed dots indicating that they were [*PSI*$^+$].

Since the pink *versus* white color of sectoring colonies could not be definitely distinguished due to the distraction of the many large red sectors, these colonies were subcloned and the variant types were determined by looking at the colony colors of non-red daughter cells (Fig. 1b and c). Although low or very high [*PIN*$^+$] variants destabilize weak [*PSI*$^+$] [47], the level of destabilization did not prevent us from scoring weak [*PSI*$^+$] colonies. A minority of sectoring colonies gave rise to both white and pink colonies. The data showed that the very high [*PIN*$^+$] variant seeded strong [*PSI*$^+$] more frequently than weak [*PSI*$^+$], while low and high [*PIN*$^+$] seeded weak [*PSI*$^+$] more frequently than strong [*PSI*$^+$].

[*PIN*$^+$] variants make variant-specific fibers *in vitro*

To determine if cellular factors were involved in the above variant-specific *in vivo* result, we asked if the same result could be obtained by cross-seeding recombinant Sup35-NM (1–254) with *in vitro* made low, high, and very high [*PIN*$^+$] specific fibers. To do this, the first step was to obtain variant-specific [*PIN*$^+$] fibers. Previous work suggested that this should be possible: crude cell extracts from [*PIN*$^+$] variants retained variant-specific infectivity when transformed into [*pin*$^-$] yeast; [75] *in vitro* made amyloid-like aggregates of Rnq1 (132–405) protein were shown to transform [*pin*$^-$] yeast into [*PIN*$^+$]; [75] Rnq1 (132–405) protein that formed fibers *in vitro* at 4 °C *versus* 37 °C gave rise to distinct [*PIN*$^+$] variants when transformed into [*pin*$^-$] yeast [76].

To obtain low, high, and very high [*PIN*$^+$] specific seed, we purified a STREP-His tap-tagged Rnq1 (132–405) construct expressed in the respective [*PIN*$^+$] variant cells (and [*pin*$^-$] as control). As expected, these seeds transformed [*pin*$^-$] cells into [*PIN*$^+$] and were variant specific. The seeds were next used to promote the *in vitro* polymerization of recombinant Rnq1 (132–405) protein. As expected for a self-seeding protein, the addition of the [*PIN*$^+$] seed significantly shortened the lag phase that proceeded exponential polymerization and led to a larger plateau value (Fig. 2). Low, high, and very high [*PIN*$^+$] variants are definitively differentiated by the efficiency with which they promote the formation of rings when Sup35NM-GFP is overexpressed: low [*PIN*$^+$] variant cells give rise to ~10% of the cells with ring-like aggregates, high [*PIN*$^+$] variants give rise to ~25%, and very high [*PIN*$^+$] variants give rise to ~40%. Importantly, the data for the different [*PIN*$^+$] variants contain non-overlapping error bars (Supplemental Fig. S1).

Table 1. Formation of variant-specific [*PIN*+] fibers

Rnq1 fibers seeded by [*PIN*+] variants	Low [*PIN*+]	High [*PIN*+]	Very high [*PIN*+]
% of [*PIN*+] transfectants with the phenotype of the [*PIN*+] variant used as seed	80% (*n* = 24)[a]	84% (*n* = 38)[b]	88% (*n* = 25)[c]

Rnq1 (132–405) fibers made with the indicated [*PIN*+] variant-specific seeds were transfected into [*pin*−][*psi*−] cells using the cell fusion protocol [77]. Fused cells were scored for [*PIN*+] by the Rnq1-GFP decoration and Sup35NM-GFP ring/line assays. The numbers of [*PIN*+] transfectants with each [*PIN*+] variant as determined with the Sup35NM-GFP rings/lines frequency assay are shown. Most of the transfectants showed the variant specificity of the seed that was used to make [*PIN*+] fibers.

[a] Of 24 transfectants, 19 contained Sup35NM-GFP rings at a rate characteristic of low [*PIN*+] (an average of 9.26% of the cells had rings); 5 of 24 caused more cells (an average of 20.8% corresponding to High [*PIN*+]) to have rings than expected of low [*PIN*+].

[b] Of 38 [*PIN*+] transfectants, 32 contained Sup35NM-GFP rings at a rate characteristic of high [*PIN*+] (an average of 23.43% of the cells had rings); 6 of 38 caused fewer cells (an average of 7.83% corresponding to low [*PIN*+]) to have rings.

[c] Of 25 [*PIN*+] transfectants, 22 contained Sup35NM-GFP rings at the rate characteristic of very high [*PIN*+] (an average of 39% of cells had rings); 3 of 25 caused fewer cells (an average of 14% corresponding to low [*PIN*+]) to have rings.

To confirm the variant specificities of these *in vitro* made fibers, we transfected them into [*pin*−] cells where the [*PIN*+] variant present was determined with the Sup35NM-GFP ring aggregate efficiency assay (Materials and Methods) (Table 1). More than 80% of the time, the transfectants had the [*PIN*+] variant used to seed the fiber. To confirm this scoring, we analyzed the level of aggregated Rnq1 in at least 10 representative transfectants for each variant type (Supplementary Fig. S2). In each case, the [*PIN*+] variant-specific ratio of soluble to aggregated Rnq1 protein predicted by the ring scoring method was obtained [15] (Supplementary Fig. S1).

Variant-specific [*PIN*+] fibers cross-seed [*PSI*+] variants

We previously showed that the addition of [*PIN*+] aggregates could increase the efficiency of conversion of soluble recombinant Sup35NM into amyloid *in vitro* [60]. Here, we used the variant-specific [*PIN*+] fibers made above to determine whether they would preferentially cross-seed recombinant Sup35NM protein into specific [*PSI*+] variant fibers. Increasing concentrations of [*PIN*+] seeds ranging from 10% to 50% (v/v) reduced and eventually eliminated the lag phase (Fig. 3).

Sup35NM fibers, polymerized for 14 h with 50% (v/v) of different [*PIN*+] variant-specific fiber seeds, were sonicated and transfected onto [*pin*−][*psi*−] yeast. The data show that the resulting frequencies of strong and weak [*PSI*+] transfectants did not mirror the [*PIN*+] variant-specific results found *in vivo* (Table 2 *versus* Fig. 1c).

[*PIN*+] variants have different propagon numbers

Propagons are the smallest infectious protein aggregates capable of transmitting a prion to progeny. Here, we test the hypothesis that [*PIN*+] variants with more propagons cross-seed the *de novo* appearance of [*PSI*+] more efficiently.

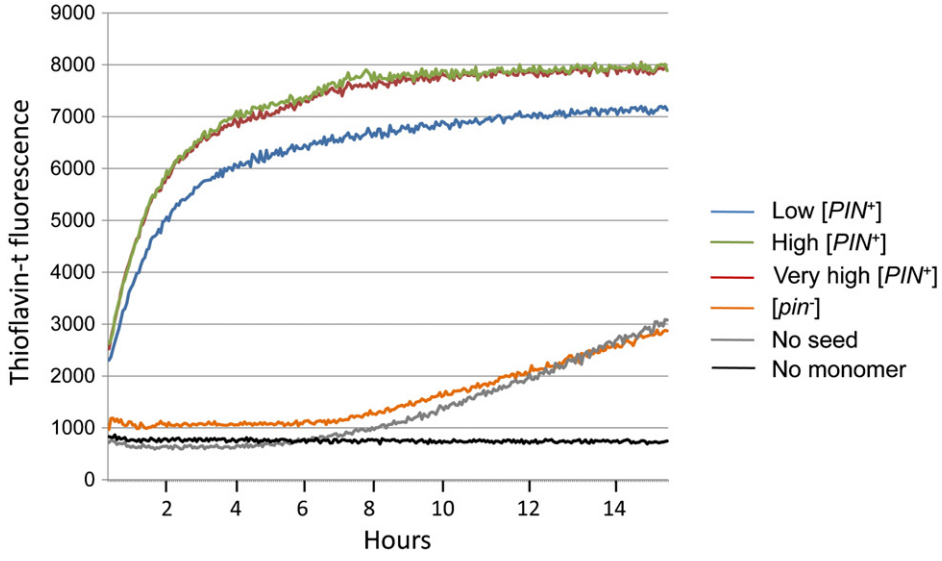


Fig. 3. Kinetics of Sup35-NM polymerization in the presence of [*PIN*+] fibers. Sup35NM or [*PSI*+] fibers were made by agitating 40 μM purified recombinant Sup35NM for 3 min every 10 s for 14 h in the presence of 50% (v/v) variant-specific sonicated [*PIN*+] fibers. Fluorescence caused by thioflavin T binding to amyloid indicates fiber formation.

Table 2. [*PSI*+] variants seeded *in vitro* with different [*PIN*+] variants

Seed	Low [*PIN*+]		High[*PIN*+]		Very high[*PIN*+]	
[*PSI*+] variant	Strong	Weak	Strong	Weak	Strong	Weak
No. of transfectants	18	10	16	20	14	18

Sup35 fibers seeded *in vitro* with the indicated [*PIN*+] variant-specific fibers were transfected into [*psi*−][*pin*−] yeast. Shown are the actual numbers of strong and weak [*PSI*+] transfectants obtained. There were no [*PSI*+] transfectants among 1000 transformants examined for Sup35NM fibers polymerized in the presence of mock "seed" isolated from [*pin*−] cells. There is no statistical difference in the *in vitro* seeding of strong *versus* weak [*PSI*+] by any of the [*PIN*+] variants.

Propagon number was estimated in different [*PIN*+] variants by following the protocol developed by Cox *et al* [78]. This protocol is based on the fact that a low concentration of GuHCl blocks the generation of new prion propagons in growing cells by inhibiting the chaperone activity of Hsp104 [35,36]. Individual cells were grown into colonies in the presence of GuHCl where the number of cells within the colony that receive a prion propagon is an estimate of the number of propagons in the initial cell. This is because while the cells in the colony keep dividing, no new prion seeds are generated. Thus, the seeds in the initial cell segregate to daughter cells in the colony and eventually many cells do not get any seed. To determine the number of cells in each colony with a seed, we spread the entire colony on medium without GuHCl so that every cell with a single seed could make more seed and give rise to a [*PRION*+] colony.

To easily score for the [*PIN*+] prion, we used the [*PIN*+] reporter protein (RRP) strain described by Bardill and True [67], where the proposed prion domain of Rnq1 (amino acids 153–405) is fused with the translation termination (MC) domain of genomic Sup35 (amino acids 124–685). This RRP chimera aggregates in response to [*PIN*+], causing nonsense suppression, which can be scored easily. We thus cytoduced low, high, and very high [*PIN*+] variants into this RRP strain. The [*PIN*+] variant-specific characteristics of the cytoductants were confirmed with both the frequency of ring appearance and Rnq1 solubility assays.

Propagon numbers were determined in 16 individual cells (from 11 cytoductants) of each variant. Low [*PIN*+] had the fewest propagons (25 ± 4.46), high [*PIN*+] had the most (96 ± 17.07), and very high [*PIN*+] had an intermediate number (average of 50 ± 5.04) (Fig. 4). This finding that very high [*PIN*+] variants have the intermediate level of propagons despite having the highest seeding efficiency among [*PIN*+] variants shows that the propagon number alone does not determine seeding efficiency. Rather differences in the seeds' conformations may determine their cross-seeding and, hence, [*PSI*+] induction efficiencies.

[*PIN*+] variants do not cause different levels of Rnq1 to be immunocaptured with Sup35 during induction of [*PSI*+]

According to the cross-seeding model, during the early stages of *de novo* [*PSI*+] formation, [*PIN*+] seeds template the aggregation of the heterologous soluble protein, Sup35. This predicts that soluble Sup35 physically interacts with the Rnq1 [*PIN*+] prion seeds [7,60,61,66]. Moreover, it seemed possible that seeds of very high [*PIN*+] variants might bind to Sup35 more efficiently than seeds of high [*PIN*+], which might bind more than seeds of low

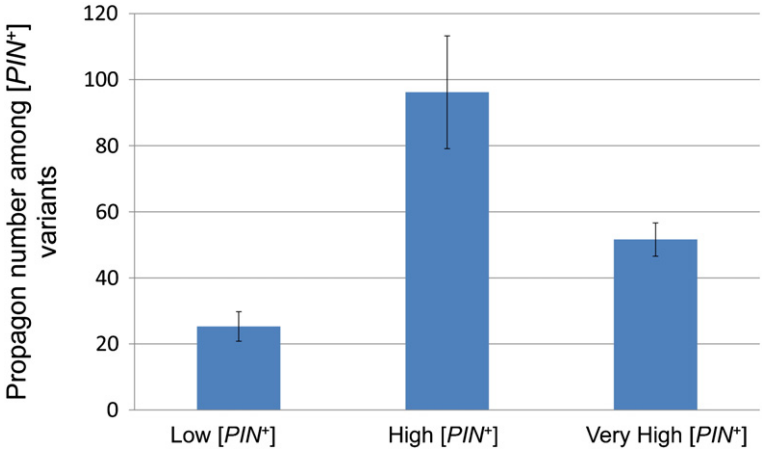


Fig. 4. Low, high, and very high [*PIN*+] variants contain different characteristic numbers of [*PIN*+] propagons. Low, high, and very high [*PIN*+] variants were cytoduced into an RRP strain (*MATa ade1-14 ura3-52 leu2-3,112 trp1-289 his3-200 sup35*::*RMC*), where [*PIN*+] cells are white, while [*pin*−] cells are red [67]. Individual cells without a bud were micromanipulated from log phase cultures of these cytoductants and grown into colonies for 48 h on medium containing 3 mM GuHCl. Each microcolony was then cut out, suspended in water, and plated on YPD without GuHCl. Cells were grown on YPD for 5 days. The number of non-red colonies arising from each microcolony on media with GuHCl was taken as the propagon number for the cell that grew into the microcolony.

[*PIN*$^+$], thereby explaining their different efficiencies in promoting [*PSI*$^+$] induction.

We used coimmunocapture experiments to test this hypothesis by comparing the level of Rnq1 associated with Sup35 in the presence of different [*PIN*$^+$] variants. We performed coimmunocapture experiments at various time points before and after the Sup35NM-GFP forms ring aggregates indicative of *de novo* [*PSI*$^+$] induction. Low, high, and very high [*PIN*$^+$] cultures transformed with p*Cup1-SUP35NM-GFP*

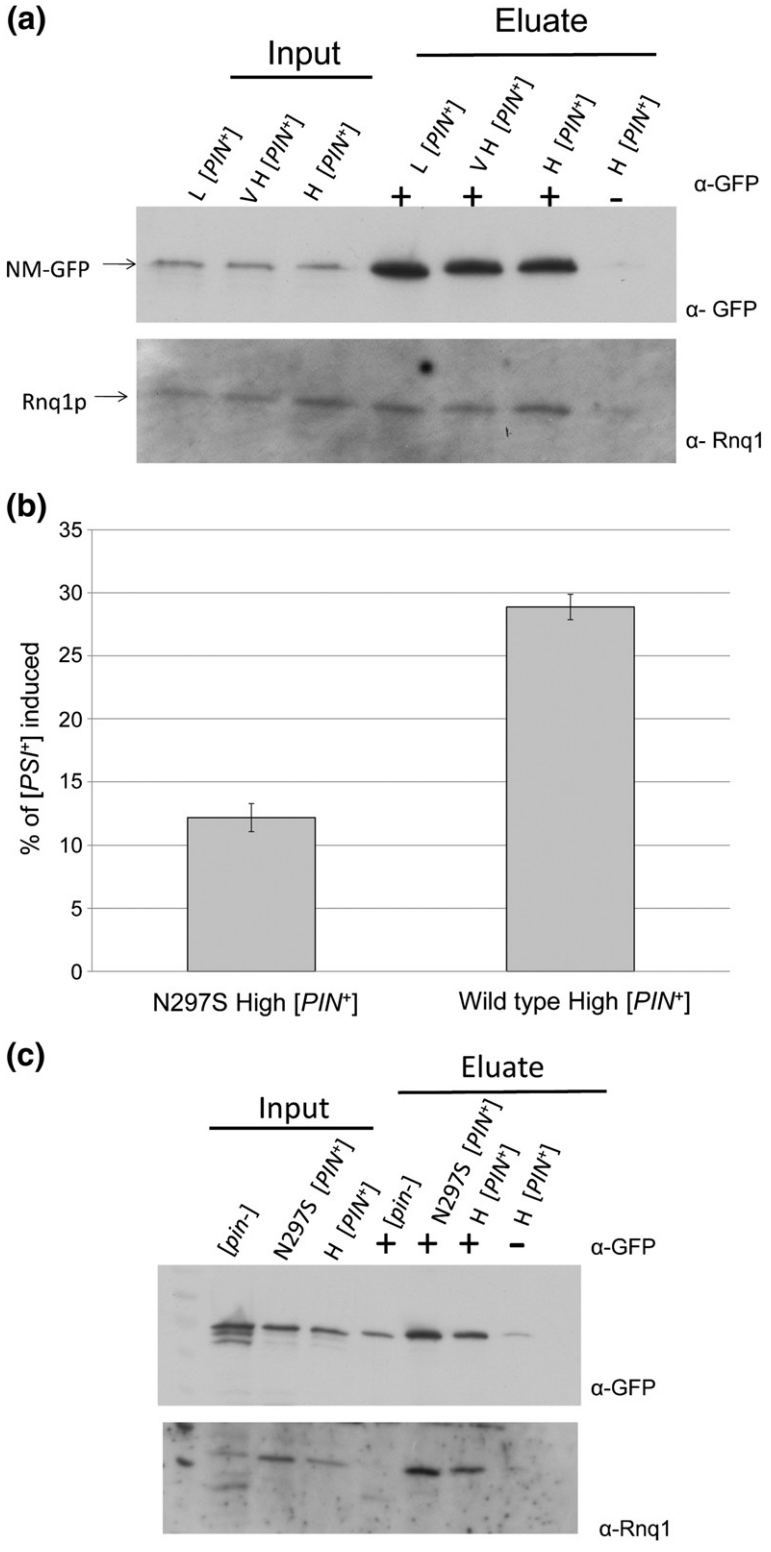


Fig. 5. Rnq1 is coimmunocaptured with Sup35 during the *de novo* induction of [*PSI*$^+$]. (a) The endogenous Rnq1 proteins in low (L), high (H), and very high (VH) [*PIN*$^+$] variants are coimmunocaptured with overexpressed Sup35 with similar efficiencies. Equal amounts of lysates from cultures with Sup35NM-GFP rings that appeared following induction of p*Cup1-SUP35NM-GFP* by growth in 50 μM copper for 20 h were immunocaptured on magnetic beads with (+) or without (–) anti-GFP antibody. Fractions eluted from the beads were analyzed by Western blot using anti-Rnq1 antibody. Input lanes show that equal amounts of crude lysates were loaded onto the columns. Eluate lanes show the level of Rnq1 specifically coimmunocaptured with Sup35-GFP in the three [*PIN*$^+$] variants. (b) A [*PIN*$^+$] strain with Rnq1 mutant, N297S, induces [*PSI*$^+$] with low frequency compared to the isogenic wild type. Overexpression of Sup35NM-GFP was induced in wild-type high [*PIN*$^+$] and mutant N297S high [*PIN*$^+$] transformed with p*Cup1-SUP35NM-GFP* by overnight growth in media containing copper. After induction, ~200 cells per plate were spread on YPD and grown for 5 days. The graph shows the total number of non-red colonies counted from four transformants of both the wild-type and mutant strain. (c) The Rnq1 mutant, N297S, does not alter the efficiency with which endogenous high [*PIN*$^+$] aggregates are coimmunocaptured with overexpressed Sup35. Sup35NM-GFP was overexpressed in high [*PIN*$^+$] with Rnq1 mutant N297S, high [*PIN*$^+$] with wild-type Rnq1, and a wild-type [*pin*$^-$] control as in (b). Immunocapture was as in (a). Shown is a representative image of six trials. There was no reproducible difference in the efficiency of coimmunocapture of mutant *versus* wild-type Rnq1 with Sup35.

were grown in 50 μM copper for 8, 15, and 20 h to induce the formation of Sup35NM-GFP rings. Sup35NM-GFP was immunocaptured with anti-GFP antibody and protein-G-labeled magnetic beads. Rnq1 was captured along with Sup35NM-GFP in all three [*PIN*$^+$] variants, but not in [*pin*$^-$] controls. This coimmunoprecipitation is dependent upon the presence of the NM-GFP aggregate since Rnq1 was not coimmunocaptured by GFP in a [*PIN*$^+$] cell expressing soluble GFP (Supplemental Fig. S3C). However, the level of coimmunocaptured Rnq1 was not reproducibly different among the three [*PIN*$^+$] variants (Fig. 5a; Supplemental Figs. S3a and S3b). Nonetheless, the association of Rnq1 with Sup35 in [*PIN*$^+$] but not [*pin*$^-$] cultures supports the cross-seeding model prediction that [*PIN*$^+$] aggregates physically interact with the heterologous Sup35 protein during induction of [*PSI*$^+$]. We also immunocaptured Rnq1 and attempted to determine the level of associated Sup35NM-GFP. However, the low level of Rnq1 *versus* the overexpressed Sup35NM-GFP caused Sup35NM-GFP to appear even in control lanes without Rnq1 antibody.

In another approach to the question of whether the interaction of [*PIN*$^+$] aggregates and Sup35 is the rate-limiting step in [*PSI*$^+$] induction, we examined the effects of a mutation in *RNQ1* (N297S) that dramatically reduces the efficiency of [*PSI*$^+$] induction [67]. Although the N297S mutation reduced the induction of [*PSI*$^+$] to less than 50% in our high [*PIN*$^+$] strain compared to the isogenic wild-type *RNQ1* high [*PIN*$^+$] strain (Fig. 5b), immunocapture of Sup35 in lysates of cells expressing the pRNQ::*RNQ1*-N297S mutant *versus* wild-type[*PIN*$^+$] aggregates showed indistinguishable levels of co-isolated Rnq1 (Fig. 5c). This again suggests that binding of Sup35 to Rnq1 [*PIN*$^+$] aggregates is not the rate-limiting step in [*PSI*$^+$] induction.

[*PIN*$^+$] variants do not differ in the levels of associated Hsp104, Sis1, and Ssa1 chaperones

We next tested whether the variant-specific [*PIN*$^+$] cross-seeding efficiencies could be caused by the binding of different levels of chaperones to [*PIN*$^+$] variant aggregates. We immunocaptured Rnq1 and compared the associated levels of the major chaperones known to participate in prion replication (Hsp104, Sis1, and Ssa1), in low, high, and very high [*PIN*$^+$] variants. We did not see any reproducible differences (Supplemental Fig. S4).

Discussion

In order to explore the mechanism by which [*PIN*$^+$] promotes the *de novo* appearance of the heterologous prion [*PSI*$^+$], we examined the genetic and biochemical properties of three distinct [*PIN*$^+$] variants. We found that each variant showed statistically different preferences for promoting the appearance of strong *versus* weak [*PSI*$^+$] variants. This result can be easily explained by the cross-seeding hypothesis. Indeed, since the structures of the different [*PIN*$^+$] seeds are presumably different, they would be expected to have different preferences for seeding weak and strong [*PSI*$^+$] variants that also have different structures.

However, this specificity was not reproduced *in vitro* when [*PIN*$^+$] variant Rnq1 fibers cross-seeded the *de novo* aggregation of Sup35. This could be due to slight differences between the *in vivo* and *in vitro* conditions such as distinctions between Rnq1 fiber ends created by sonication *versus in vivo* fiber ends made by chaperones. Possibly, cellular factors missing *in vitro* are directly involved in cross-seeding specificity, for example, chaperones that affect the conformation of cross-seeded Sup35 fibers. Indeed, Hsp70s are integral components of *in vivo* [*PSI*$^+$] prion fiber assemblies [79]. Likewise, Hsp104 enhances the ability of [*PIN*$^+$] aggregates to promote the *de novo in vivo* appearance of a heterologous prion [80].

According to the cross-seeding hypothesis, one might expect conversion of heterologous soluble Sup35 protein to occur at the [*PIN*$^+$] fiber ends. In this case, the efficiency of a [*PIN*$^+$] variant in cross-seeding the appearance of [*PSI*$^+$] should depend upon the number of Rnq1 fiber ends. Indeed, *in vitro*, the efficiency with which Rnq1 fibers promoted the conversion of soluble Sup35 to amyloid fibers was dramatically increased when the number of Rnq1 fiber ends was increased by sonication [60,61].

In vivo, the number of Rnq1 fiber ends would be expected to be proportional to the number of infectious amyloid aggregates (propagons) present in the cells. Thus, we determined the number of propagons characteristic for each of the three [*PIN*$^+$] variants. While the variants differed in propagon number, this difference did not coincide with their [*PSI*$^+$] induction efficiencies. Thus, in addition to the number of available fiber ends, it is likely that the specific fiber conformations influence the efficiencies with which the different variants template the conversion of Sup35 to amyloid. This idea is also supported by our previous finding [15] that very high [*PIN*$^+$] contains less aggregated Rnq1 than the other [*PIN*$^+$] variants and yet promotes the appearance of [*PSI*$^+$] more efficiently than the other variants.

The coimmunocapture experiments described here support the cross-seeding hypothesis that requires overexpressed Sup35NM to physically interact with Rnq1 during [*PSI*$^+$] induction. Importantly, Rnq1 was not overexpressed in our experiments and was not coimmunocaptured with Sup35 in control [*pin*$^-$] cells where [*PSI*$^+$] was not induced. However, we did not detect any differences in the level of coimmunocapture of Rnq1 with overexpressed Sup35NM in cells with low, high, or very high [*PIN*$^+$] variants despite

their distinct differences in [*PSI*$^+$] inducing capacities. Likewise, the Rnq1 mutant, N297S, which causes a 50% reduction in the efficiency with which [*PIN*$^+$] induces [*PSI*$^+$], did not cause a reduction in coimmunocapture of Rnq1 with Sup35. While transient or *in vivo* binding might not be detected by coimmunocapture, the simplest interpretation of the results is that the different [*PSI*$^+$] induction efficiencies of the [*PIN*$^+$] variants and the *RNQ1-N297S* mutant are not caused by different levels of Rnq1 binding to Sup35. It thus appears that while the promotion of the appearance of [*PSI*$^+$] by [*PIN*$^+$] requires Sup35 to interact with Rnq1, this is not sufficient. We propose that, following binding, there is an additional interaction step when the actual conversion of soluble Sup35 to aggregated Sup35 occurs and that this is the point where [*PIN*$^+$] aggregates differentially catalyze the Sup35 to [*PSI*$^+$] conversion as per their variant specificity. Similar mechanisms may explain the ability of heterologous amyloid aggregates in mammals to enhance the *de novo* appearance of amyloid associated with disease [70,81].

Materials and Methods

Yeast strains, plasmids, and media

The yeast strains used in this study are listed in Table 3. Many are derivatives of 74-D694 (*MATa ade1-14 ura3-52 leu2-3, 112 trp1-289 his3-200*) [82]. Yeast was grown at 30 °C unless otherwise indicated. Media were as described previously [83]. YPD is a complex medium that contains 2% dextrose and is used to grow yeast and distinguish yeast prion variants. Synthetic dextrose medium lacks one or more amino acid (e.g., medium lacking leucine is called –Leu) to select for appropriate plasmids or to select for diploid strains. YPG is a complex medium that contains 3% glycerol and is used to select against mitochondrial mutants (petites). To express genes under the *GAL* inducible promoter, we used 2% raffinose and 2% galactose as the sugar source. YPD containing 5 mM GuHCl was used for [*PSI*$^+$] curing experiments.

Plasmid, p*Cup1-SUP35NM-GFP* (p1182, *CEN2 LEU2*), containing a copper-inducible promoter and the prion and middle domains of Sup35 (Sup35NM) fused to green fluorescent protein was used to induce [*PSI*$^+$] in various [*PIN*$^+$] backgrounds [64]. The 2 μ plasmid p*GAL*::*SUP35C* (p1598) carries Sup35C under the *GAL* promoter and the *TRP1* selective marker [73]. Plasmid p*Cup1*::*RNQ1GFP*, *HIS3* (pID116; kindly supplied by Irina Derkatch) was used to express wild-type, full-length Rnq1-GFP to stain [*PIN*$^+$] aggregates in the Rnq1 decoration assay (see below). Plasmid p*RNQ*::*RNQ1*-N297S (p1862) carrying the Rnq1 mutation, N297S, at the C-terminal end and the *HIS3* selective marker in a pRS313 backbone was a kind gift from H. True [67]. The N297S mutation considerably reduces the efficiency with which [*PIN*$^+$] facilitates the induction of [*PSI*$^+$]. His-tagged proteins *His$_{10}$-RNQ1PD* (amino acids 132–405) and *His$_{10}$-SUP35NM* (amino acids 1–254) were respectively expressed in plasmids p1510 and p1195, with the pJC45 expression vector backbone [75,84,85]. Wild-type *RNQ1PD* (131–405) was amplified from p1415 (p*Cup1-RNQ1*::*GFP*), cut with BamHI and SacI, and ligated into p*Cup1-GFP*, *URA3* (p984) [86] also cut with BamHI and SacI to create p*Cup1*:*His$_{10}$ RNQ1PD GFP StrepII* (p1866) with a *URA3* marker.

[*PSI*$^+$] color assay

All yeast strains used in this study have the *ade1-14* allele that has a nonsense mutation and is frequently used to score for [*PSI*$^+$] [33]. In [*psi*$^-$] cells, Sup35 functions as a translation termination factor essential for terminating translation at stop codons including the premature *ade1-14* nonsense codon. This causes *ade1-14* [*psi*$^-$] cells to be Ade$^-$ and to accumulate red pigment on rich medium such as YPD. In contrast, in [*PSI*$^+$] cells, where Sup35 is aggregated and is not fully functional, there is occasional read through of the *ade1-14* premature stop codon; hence, some full-length Ade1 is synthesized, giving Ade$^+$ non-red colonies. When the *ade1-14* mutation is efficiently suppressed, for example, by strong [*PSI*$^+$], cells return to their white color, while weak [*PSI*$^+$] causes inefficient suppression and a pink colony color. We confirmed that the presence of p*GAL*::*SUP35C* plasmid did not alter the colony color.

[*PSI*$^+$] Sup35NM-GFP and [*PIN*$^+$] Rnq1-GFP decoration assays

When Sup35NM-GFP is expressed in [*PSI*$^+$] cells, it decorates the [*PSI*$^+$] aggregates and can be seen as fluorescent dots within a few hours. In contrast, in [*psi*$^-$] cells, Sup35NM-GFP remains diffuse [64]. Cells to be scored for [*PSI*$^+$] by this assay are sometimes directly transformed with the p*Cup1-SUP35NM-GFP* plasmid and other times are crossed with a [*psi*$^-$][*pin*$^-$] strain bearing the plasmid.

Table 3. Yeast strains used in this study

Strains	Description	Source
L1749	*MATa ade1-14 ura3-52 leu2-3, 112 trp1-289 his3-200* [*psi*$^-$] High [*PIN*$^+$] [*PIN*$^+$]	Ref. [32]
L1943	*MATa ade1-14 ura3-52 leu2-3,112 trp1-289 his3-200* [*psi*$^-$] Low [*PIN*$^+$] [*PIN*$^+$]	Ref. [15]
L1953	*MATa ade1-14 ura3-52 leu2-3,112 trp1-289 his3-200* [*psi*$^-$] Very high [*PIN*$^+$] [*PIN*$^+$]	Ref. [15]
L2910	*MATa ade1-14 ura3-52 leu2-3,112 trp1-289 his3-200* [*psi*$^-$][*pin*$^-$]	Ref. [32]
L2731	*MATa ade1-14 ura3-52 leu2-3,112 trp1-289 his3-200 HIS3-Gal::SUP35* [*psi*$^-$][*pin*$^-$]	Ref. [73]
GF837	*MATa ade1-14 ura3-52 leu2-3,112 trp1-289 his3-200,sup35::RMC*	Ref. [67]
GF840	*MATα ade1-14 ura3-52 leu2-3,112 trp1-289 his3-200,rnq1::KanMx4* [*psi*$^-$] High [*PIN*$^+$]	Ref. [67]
L2642	*MATα ade1-14 ura3-52 leu2-3,112 trp1-289 lys9-A21* [*psi*$^-$][*pin*$^-$]	Ref. [32]
GF585	*MATα ade1-14 trp1-289 his3-delta200 ura3-52 leu2-3, 112* [*psi*$^-$][*pin*$^-$]	Ref. [33]

Transformants or diploids were examined with a fluorescent microscope after overnight growth in 50 μM Cu. Analogous assays were done for [*PIN*$^+$] using Rnq1-GFP.

Preparation of [*PIN*$^+$] variant-specific seeds from yeast

[*PIN*$^+$] variant-specific seeds were prepared by inducing expression of tap-tagged Rnq1 with 50 μM copper in [*PIN*$^+$] and [*pin*$^-$] cells transformed with p*CUP-HIS*$_{10}$*RNQ1*(*132–405*)*-GFP STREP II*. After overnight induction, cells were harvested and His-tagged Rnq1 (132–405) aggregates were purified with Ni-NTA agarose affinity column chromatography (Qiagen) following the manufacturer's native conditions instructions. The concentration of protein purified from all [*PIN*$^+$] variants and [*pin*$^-$] was normalized to 6–8 μg/μl for use in seeding reactions of Rnq1 PD.

Recombinant protein expression and purification

His$_{10}$Sup35-NM (1–254) was induced in *Escherichia coli* (BL21DE3) transformed with p1195 by the addition of 1 mM IPTG to cultures growing at 37 °C [84]. The bacteria were lysed by sonicating (Branson) cells for 20 s with 1 min incubation in ice 5× in 20 mM Tris–HCl and 8 M urea (pH 8.0). Likewise, His$_{10}$Rnq1-PD (132–405) was induced in *E. coli* (BL21 AI) transformed with p1510 by the addition of 1 mM IPTG together with 0.15% (w/v) L(+) arabinose [75]. Lysis was as above but in 100 mM NaH_2PO_4, 10 mM Tris–Cl, and 8 M urea (pH 8.0).

Both the recombinant proteins were purified from lysed cells with Ni-NTA agarose affinity column chromatography (Qiagen) under denaturing conditions in 8 M urea following the manufacturer's instructions and were stored at −80°C.

In vitro aggregation of Rnq1 (132–405) and Sup35NM

Denatured Rnq1 (132–405) stored in 8 M urea was diluted to 40–60 μM in aggregation buffer [100 mM sodium phosphate (pH 7.3), 4 M urea, and 1 M NaCl] [60,75]. Thioflavin T dye stock of 5 mM was added to 125 μl of the reaction mixture in a 96-well plate. The microplate was incubated for up to 48 h in a Spectramax-Max microplate reader at 30 °C. The plate was shaken intermittently for 10 s every 3 min and aggregation was monitored by fluorescence using an excitation wavelength of 450 nm and an emission wavelength of 482 nm. The reactions were seeded with 8% (v/v) sonicated (10 s at 15% power) seeds purified from cells with the different [*PIN*$^+$] variants.

The above protocol was also followed for Sup35NM polymerization, except that level of [*PIN*$^+$] seed was increased. Here, 10–50% (v/v) of sonicated (10 s at 15% power) preformed [*PIN*$^+$] fibers were added to the reaction mixture and fluorescence recorded.

[*PIN*$^+$] transfection

The protocol described in Ref. [77] for transfection of Sup35 fibers was modified slightly to allow transfection of *in vitro* made Rnq1 fibers. Yeast (L2642 and GF585) of the same mating type, but with complementary markers, were harvested at mid log phase and were separately converted into spheroplasts by lyticase treatment. The two spheroplast populations were incubated with Rnq1 fibers and then combined. This mixture was plated on medium that selects for fused cells (−His–Lys). Colonies of the fused cells were first screened for the presence of the [*PIN*$^+$] prion by mating each of them with a *MAT*a [*pin*$^-$] strain carrying the p*Cup1-RNQ1-GFP* plasmid. The unmated fused cells corresponding to the triploids that showed fluorescent dots after overnight growth in 50 μM Cu were transformed with the p*Cup1-SUP35NM-GFP* plasmid to enable scoring of the specific [*PIN*$^+$] variant present *via* the Sup35NM-GFP ring induction method (see below).

Distinguishing [*PIN*$^+$] variants by the frequency of Sup35NM-GFP rings/lines

Overexpression of p*Cup1-SUP35NM-GFP* in a [*PIN*$^+$] [*psi*$^-$] background gives rise to cells with ring- or line-like aggregates indicative of [*PSI*$^+$] induction [64]. Furthermore, the frequency of the ring/line aggregates is different for each of the [*PIN*$^+$] variants used here. After 20-h induction of Sup35NM-GFP, [*pin*$^-$] cultures showed essentially no cells with rings/lines; low [*PIN*$^+$] cultures had ~10% of cells with rings/lines; high [*PIN*$^+$] cultures had ~25% of cells with rings/lines, and very high [*PIN*$^+$] cultures had ~40% of cells with rings/lines (Supplemental Fig. S1).

Distinguishing [*PIN*$^+$] variants on the basis of Rnq1 solubility

The solubility of Rnq1 was assayed essentially as described previously [13]. [*PIN*$^+$] variants differ in the levels of soluble *versus* aggregated Rnq1 present in the cell: very high [*PIN*$^+$] has more soluble Rnq1 than low [*PIN*$^+$], which has more soluble Rnq1 than high [*PIN*$^+$] (Supplemental Fig. S2) [15]. To determine the levels of soluble *versus* aggregated Rnq1, we resuspended 50 ml of log phase washed cells in 750 μl of lysis buffer [50 mM KCl, 10 mM $MgCl_2$, 50 mM Tris–HCl, pH 7.5, and 5% (wt/vol) glycerol, 1:50 diluted protease inhibitor cocktail (Sigma, St. Louis, MO), and 5 mM PMSF], mixed them with 750 μl of 0.5-mm glass beads (Biospec, Bartlesville, OK), and lysed them by vortexing at high speed for 1 min/5×, with 1 min cooling on ice after each vortexing. Cell debris was removed by centrifuging twice at 600*g* for 1 min. Supernatant and pellet fractions of lysates were separated by centrifugation at 80,000 rpm for 30 min in a Sorvall TLA100.1 rotor at 4 °C. The total, supernatant, and pellet (resuspended in 250 μl of lysis buffer) fractions were resolved on 10% polyacrylamide gels that were transferred to a polyvinylidene difluoride membrane and probed with polyclonal Rnq1 antibody (kind gift from S. Lindquist).

[*PSI*$^+$] transfection and scoring of [*PSI*$^+$] transfectants

Sup35NM fibers were transfected as described previously [87]. The *in vitro* made amyloid aggregates of recombinant Sup35NM were transformed into [*psi*$^-$][*pin*$^-$] spheroplasts in the presence of the p*Cup1-SUP35NM-GFP,LEU2* plasmid. Leu$^+$ transformants were patched on YPD medium and grown for 3 days, and the color was examined to score for [*psi*$^-$] (red), weak [*PSI*$^+$] (pink), and strong [*PSI*$^+$] (white) as described above in [*PSI*$^+$] color assay. All Leu$^+$ transformants with non-red phenotypes were tested for [*PSI*$^+$] with the SUP35NM-GFP aggregate decoration assay (see

above), by growing cells overnight in –Leu with 50 μM copper to induce Sup35NM-GFP. Some transformants were further confirmed to be [*PSI*+] by subcloning them on 5 mM GuHCl to test for GuHCl curability. Red colonies were restreaked on YPD to confirm they were cured by the reappearance of red colony color [88,89].

Counting [*PIN*+] propagons

The method previously used to count [*PSI*+] propagons [78] was modified for [*PIN*+]. To easily score for [*PIN*+], we used strains carrying the RRP Rnq1 prion domain fused to Sup35MC. In the absence of [*PIN*+], these strains are red. However, in the presence of [*PIN*+], they are white or pink on –Ade, indicative of nonsense suppression [67]. Individual RRP cells with the different [*PIN*+] variants were micromanipulated from log phase cultures to a 2% noble agar pad that was then placed on a YPD plate containing 3 mM GuHCl and grown for 48 h. The whole colony was then cut out of the pad, suspended in water, and spread on YPD where the number of non-red colonies was taken as the propagon number in the initial cell.

Immunoprecipitation

For the pull-down assays, the μ MACS protein MicroBeads isolation kit was used (Miltenyi Biotec, Auburn, CA). Reactions containing 0.25–1 μg/μl of sample protein were incubated with or without anti-GFP antibody for 2 h. Then, 50 μl of protein-G-labeled micro beads (Miltenyi Biotec) was added and the reactions were mixed and incubated for 30 min on ice. Samples were loaded on magnetic separation μ Columns (Miltenyi Biotec), washed 5× with buffer, and eluted in heated 1× sample buffer containing 2% SDS [90]. Eluate (30–40 μl) was run on 10% polyacrylamide gels (Bio-Rad), transferred to polyvinylidine dihydrofluoride membrane (Bio-Rad), and probed for specific proteins. Anti-GFP antibody was from Roche Applied Science (Indianapolis, IN). Anti-Sup35C antibody developed by Dr. V. Prapapanich (BE4 mouse monoclonal antibodies) was used to detect Sup35 protein. Anti-Rnq1 antibody was a kind gift from Dr. S. Lindquist.

Supplementary data to this article can be found online at http://dx.doi.org/10.1016/j.jmb.2013.06.006

Acknowledgements

We thank Dr. S. Lindquist (Massachusetts Institute of Technology) for Rnq1 antibody, Dr. H. True (Washington University School of Medicine) for the RRP strain and the p*RNQ*::*RNQ1*-N297S plasmid, and Dr. V. Kanneganti (University of Nevada, Reno) for helpful comments on the manuscript. This work was supported by National Institutes of Health Grant R01GM056350 to S.W.L. The content of this article is solely the responsibility of the authors and does not necessarily represent the official views of the National Institutes of Health.

Conflict of Interest Statement. The authors declare that they have no conflict of interest.

Received 4 February 2013;
Received in revised form 7 May 2013;
Accepted 7 June 2013
Available online 14 June 2013

Keywords
Prion;
Sup35;
PSI+;
PIN+;
Yeast

Abbreviations used:
PrP, prion protein; RRP, Rnq1 reporter protein; YPD, yeast extract, peptone, dextrose; Aβ, amyloid beta-protein; GuHCl, guanidine hydrochloride.

References

[1] Prusiner SB. Prions. Proc Natl Acad Sci USA 1998;95:13363–83.
[2] Pan KM, Baldwin M, Nguyen J, Gasset M, Serban A, Groth D, et al. Conversion of alpha-helices into beta-sheets features in the formation of the scrapie prion proteins. Proc Natl Acad Sci USA 1993;90:10962–6.
[3] Fraser H, Dickinson AG. Scrapie in mice. Agent-strain differences in the distribution and intensity of grey matter vacuolation. J Comp Pathol 1973;83:29–40.
[4] Collinge J, Sidle KC, Meads J, Ironside J, Hill AF. Molecular analysis of prion strain variation and the aetiology of 'new variant' CJD. Nature 1996;383:685–90.
[5] Bessen RA, Marsh RF. Distinct PrP properties suggest the molecular basis of strain variation in transmissible mink encephalopathy. J Virol 1994;68:7859–68.
[6] Soto C. Unfolding the role of protein misfolding in neurodegenerative diseases. Nat Rev Neurosci 2003;4:49–60.
[7] Derkatch IL, Bradley ME, Hong JY, Liebman SW. Prions affect the appearance of other prions: the story of [PIN(+)]. Cell 2001;106:171–82.
[8] Du Z, Park K-W, Yu H, Fan Q, Li L. Newly identified prion linked to the chromatin-remodeling factor Swi1 in *Saccharomyces cerevisiae*. Nat Genet 2008;40:460–5.
[9] Patel BK, Gavin-Smyth J, Liebman SW. The yeast global transcriptional co-repressor protein Cyc8 can propagate as a prion. Nat Cell Biol 2009;11:344–9.
[10] Wickner RB. [URE3] as an altered URE2 protein: evidence for a prion analog in *Saccharomyces cerevisiae*. Science 1994;264:566–9.
[11] Cox BS. [PSI], a cytoplasmic suppressor of super-suppressors in yeast. Heredity 1965;20:505–21.
[12] Alberti S, Halfmann R, King O, Kapila A, Lindquist S. A systematic survey identifies prions and illuminates sequence features of prionogenic proteins. Cell 2009;137:146–58.
[13] Sondheimer N, Lindquist S. Rnq1: an epigenetic modifier of protein function in yeast. Mol Cell 2000;5:163–72.
[14] Derkatch IL, Chernoff YO, Kushnirov VV, Inge-Vechtomov SG, Liebman SW. Genesis and variability of [PSI] prion factors in *Saccharomyces cerevisiae*. Genetics 1996;144:1375–86.

[15] Bradley ME, Edskes HK, Hong JY, Wickner RB, Liebman SW. Interactions among prions and prion "strains" in yeast. Proc Natl Acad Sci USA 2002;99:16392–9.
[16] Schlumpberger M, Prusiner SB, Herskowitz I. Induction of distinct [URE3] yeast prion strains. Mol Cell Biol 2001;21: 7035–46.
[17] Tanaka M, Collins SR, Toyama BH, Weissman JS. The physical basis of how prion conformations determine strain phenotypes. Nature 2006;442:585–9.
[18] Krishnan R, Lindquist SL. Structural insights into a yeast prion illuminate nucleation and strain diversity. Nature 2005;435:765–72.
[19] Oesch B, Westaway D, Walchli M, McKinley MP, Kent SB, Aebersold R, et al. A cellular gene encodes scrapie PrP 27–30 protein. Cell 1985;40:735–46.
[20] Masison DC, Wickner RB. Prion-inducing domain of yeast Ure2p and protease resistance of Ure2p in prion-containing cells. Science 1995;270:93–5.
[21] Ter-Avanesyan MD, Kushnirov VV, Dagkesamanskaya AR, Didichenko SA, Chernoff YO, Inge-Vechtomov SG, Smirnov VN. Deletion analysis of the SUP35 gene of the yeast *Saccharomyces cerevisiae* reveals two non-overlapping functional regions in the encoded protein. Mol Microbiol 1993;7:683–92.
[22] Cohen FE, Prusiner SB. Pathologic conformations of prion proteins. Annu Rev Biochem 1998;67:793–819.
[23] Wickner RB, Liebman SW, Saupe SJ. Chapter 7 "Prions of Yeast and Filamentous Fungi: [URE3+], [PSI+], [PIN+], and [Het-s]", Second edit. In: Prusiner SB, editor. Prion Biology and Diseases. Cold Spring Harbor, NY: Cold Spring Harbor Laboratory Press; 2004. p. 305–78.
[24] Liebman SW, Chernoff YO. Prions in yeast. Genetics 2012;191:1041–72.
[25] Tuite MF, Marchante R, Kushnirov V. Fungal prions: structure, function and propagation. Top Curr Chem 2011;305:257–98.
[26] Wickner RB, Edskes HK, Kryndushkin D, McGlinchey R, Bateman D, Kelly A. Prion diseases of yeast: amyloid structure and biology. Semin Cell Dev Biol 2012;22:469–75.
[27] Kryndushkin DS, Alexandrov IM, Ter-Avanesyan MD, Kushnirov VV. Yeast [PSI+] prion aggregates are formed by small Sup35 polymers fragmented by Hsp104. J Biol Chem 2003;278:49636–43.
[28] Shorter J, Lindquist S. Hsp104 catalyzes formation and elimination of self-replicating Sup35 prion conformers. Science 2004;304:1793–7.
[29] Higurashi T, Hines JK, Sahi C, Aron R, Craig EA. Specificity of the J-protein Sis1 in the propagation of 3 yeast prions. Proc Natl Acad Sci USA 2008;105:16596–601.
[30] Tipton KA, Verges KJ, Weissman JS. In vivo monitoring of the prion replication cycle reveals a critical role for Sis1 in delivering substrates to Hsp104. Mol Cell 2008;32: 584–91.
[31] Tuite MF, Serio TR. The prion hypothesis: from biological anomaly to basic regulatory mechanism. Nat Rev Mol Cell Biol 2010;11:823–33.
[32] Derkatch IL, Bradley ME, Zhou P, Chernoff YO, Liebman SW. Genetic and environmental factors affecting the de novo appearance of the [PSI+] prion in *Saccharomyces cerevisiae*. Genetics 1997;147:507–19.
[33] Chernoff YO, Lindquist SL, Ono B, Inge-Vechtomov SG, Liebman SW. Role of the chaperone protein Hsp104 in propagation of the yeast prion-like factor [psi+]. Science 1995;268:880–4.
[34] Moriyama H, Edskes HK, Wickner RB. [URE3] prion propagation in *Saccharomyces cerevisiae*: requirement for chaperone Hsp104 and curing by overexpressed chaperone Ydj1p. Mol Cell Biol 2000;20:8916–22.
[35] Jung G, Masison DC. Guanidine hydrochloride inhibits Hsp104 activity in vivo: a possible explanation for its effect in curing yeast prions. Curr Microbiol 2001;43:7–10.
[36] Ferreira PC, Ness F, Edwards SR, Cox BS, Tuite MF. The elimination of the yeast [PSI+] prion by guanidine hydrochloride is the result of Hsp104 inactivation. Mol Microbiol 2001;40:1357–69.
[37] Wickner RB, Masison DC, Edskes HK. [PSI] and [URE3] as yeast prions. Yeast 1995;11:1671–85.
[38] Stansfield I, Jones KM, Kushnirov VV, Dagkesamanskaya AR, Poznyakovski AI, Paushkin SV, et al. The products of the SUP45 (eRF1) and SUP35 genes interact to mediate translation termination in *Saccharomyces cerevisiae*. EMBO J 1995;14:4365–73.
[39] Vitrenko YA, Pavon ME, Stone SI, Liebman SW. Propagation of the [PIN+] prion by fragments of Rnq1 fused to GFP. Curr Genet 2007;51:309–19.
[40] Kadnar ML, Articov G, Derkatch IL. Distinct type of transmission barrier revealed by study of multiple prion determinants of Rnq1. PLoS Genet 2010;6:e1000824.
[41] Bradley ME, Liebman SW. The Sup35 domains required for maintenance of weak, strong or undifferentiated yeast [PSI+] prions. Mol Microbiol 2004;51:1649–59.
[42] Hosoda N, Kobayashi T, Uchida N, Funakoshi Y, Kikuchi Y, Hoshino S, Katada T. Translation termination factor eRF3 mediates mRNA decay through the regulation of deadenylation. J Biol Chem 2003;278:38287–91.
[43] Ter-Avanesyan MD, Dagkesamanskaya AR, Kushnirov VV, Smirnov VN. The SUP35 omnipotent suppressor gene is involved in the maintenance of the non-Mendelian determinant [psi+] in the yeast *Saccharomyces cerevisiae*. Genetics 1994;137:671–6.
[44] Liu JJ, Sondheimer N, Lindquist SL. Changes in the middle region of Sup35 profoundly alter the nature of epigenetic inheritance for the yeast prion [PSI+]. Proc Natl Acad Sci USA 2002;99:16446–53.
[45] Cox BS, Tuite MF, McLaughlin CS. The psi factor of yeast: a problem in inheritance. Yeast 1988;4:159–78.
[46] Zhou P, Derkatch IL, Uptain SM, Patino MM, Lindquist S, Liebman SW. The yeast non-Mendelian factor [ETA+] is a variant of [PSI+], a prion-like form of release factor eRF3. EMBO J 1999;18:1182–91.
[47] Bradley ME, Liebman SW. Destabilizing interactions among [PSI(+)] and [PIN(+)] yeast prion variants. Genetics 2003;165:1675–85.
[48] Uptain SM, Sawicki GJ, Caughey B, Lindquist S. Strains of [PSI(+)] are distinguished by their efficiencies of prion-mediated conformational conversion. EMBO J 2001;20:6236–45.
[49] Kochneva-Pervukhova NV, Chechenova MB, Valouev IA, Kushnirov VV, Smirnov VN, Ter-Avanesyan MD. [Psi(+)] prion generation in yeast: characterization of the 'strain' difference. Yeast 2001;18:489–97.
[50] Alexandrov IM, Vishnevskaya AB, Ter-Avanesyan MD, Kushnirov VV. Appearance and propagation of polyglutamine-based amyloids in yeast: tyrosine residues enable polymer fragmentation. J Biol Chem 2008;283:15185–92.
[51] Verges KJ, Smith MH, Toyama BH, Weissman JS. Strain conformation, primary structure and the propagation of the yeast prion [PSI+]. Nat Struct Mol Biol 2011;18:493–9.
[52] Toyama BH, Kelly MJ, Gross JD, Weissman JS. The structural basis of yeast prion strain variants. Nature 2007;449:233–7.
[53] DiSalvo S, Derdowski A, Pezza JA, Serio TR. Dominant prion mutants induce curing through pathways that promote

chaperone-mediated disaggregation. Nat Struct Mol Biol 2011;18:486–92.
[54] Cox BS, Byrne LJ, Tuite MF. Prion stability. Prion 2007;1:170–8.
[55] King CY. Supporting the structural basis of prion strains: induction and identification of [PSI] variants. J Mol Biol 2001;307:1247–60.
[56] Lin JY, Liao TY, Lee HC, King CY. Inter-allelic prion propagation reveals conformational relationships among a multitude of [PSI] strains. PLoS Genet 2011;7:e1002297.
[57] Toyama BH, Weissman JS. Amyloid structure: conformational diversity and consequences. Annu Rev Biochem 2011;80:557–85.
[58] Derkatch IL, Bradley ME, Masse SV, Zadorsky SP, Polozkov GV, Inge-Vechtomov SG, Liebman SW. Dependence and independence of [PSI(+)] and [PIN(+)]: a two-prion system in yeast? EMBO J 2000;19:1942–52.
[59] Osherovich LZ, Weissman JS. Multiple Gln/Asn-rich prion domains confer susceptibility to induction of the yeast [PSI(+)] prion. Cell 2001;106:183–94.
[60] Vitrenko YA, Gracheva EO, Richmond JE, Liebman SW. Visualization of aggregation of the Rnq1 prion domain and cross-seeding interactions with Sup35NM. J Biol Chem 2007;282:1779–87.
[61] Derkatch IL, Uptain SM, Outeiro TF, Krishnan R, Lindquist SL, Liebman SW. Effects of Q/N-rich, polyQ, and non-polyQ amyloids on the de novo formation of the [PSI+] prion in yeast and aggregation of Sup35 in vitro. Proc Natl Acad Sci USA 2004;101:12934–9.
[62] Bagriantsev S, Liebman SW. Specificity of prion assembly in vivo. [PSI+] and [PIN+] form separate structures in yeast. J Biol Chem 2004;279:51042–8.
[63] Salnikova AB, Kryndushkin DS, Smirnov VN, Kushnirov VV, Ter-Avanesyan MD. Nonsense suppression in yeast cells overproducing Sup35 (eRF3) is caused by its non-heritable amyloids. J Biol Chem 2005;280:8808–12.
[64] Zhou P, Derkatch IL, Liebman SW. The relationship between visible intracellular aggregates that appear after overexpression of Sup35 and the yeast prion-like elements [PSI(+)] and [PIN(+)]. Mol Microbiol 2001;39:37–46.
[65] Mathur V, Taneja V, Sun Y, Liebman SW. Analyzing the birth and propagation of two distinct prions, [PSI+] and [Het-s](y), in yeast. Mol Biol Cell 2010;21:1449–61.
[66] Choe YJ, Ryu Y, Kim HJ, Seok YJ. Increased [PSI+] appearance by fusion of Rnq1 with the prion domain of Sup35 in *Saccharomyces cerevisiae*. Eukaryot Cell 2009;8:968–76.
[67] Bardill JP, True HL. Heterologous prion interactions are altered by mutations in the prion protein Rnq1p. J Mol Biol 2009;388:583–96.
[68] Johan K, Westermark G, Engstrom U, Gustavsson A, Hultman P, Westermark P. Acceleration of amyloid protein A amyloidosis by amyloid-like synthetic fibrils. Proc Natl Acad Sci USA 1998;95:2558–63.
[69] O'Nuallain B, Williams AD, Westermark P, Wetzel R. Seeding specificity in amyloid growth induced by heterologous fibrils. J Biol Chem 2004;279:17490–9.
[70] Morales R, Estrada LD, Diaz-Espinoza R, Morales-Scheihing D, Jara MC, Castilla J, Soto C. Molecular cross talk between misfolded proteins in animal models of Alzheimer's and prion diseases. J Neurosci 2010;30:4528–35.
[71] Gotz J, Chen F, van Dorpe J, Nitsch RM. Formation of neurofibrillary tangles in P301l tau transgenic mice induced by Abeta 42 fibrils. Science 2001;293:1491–5.
[72] Lasagna-Reeves CA, Castillo-Carranza DL, Guerrero-Muoz MJ, Jackson GR, Kayed R. Preparation and characterization of neurotoxic tau oligomers. Biochemistry 2010;49:10039–41.
[73] Vishveshwara N, Bradley ME, Liebman SW. Sequestration of essential proteins causes prion associated toxicity in yeast. Mol Microbiol 2009;73:1101–14.
[74] Sharma J, Liebman SW. [PSI(+)] prion variant establishment in yeast. Mol Microbiol 2012.
[75] Patel BK, Liebman SW. "Prion-proof" for [PIN+]: infection with in vitro-made amyloid aggregates of Rnq1p-(132–405) induces [PIN+]. J Mol Biol 2007;365:773–82.
[76] Kalastavadi T, True HL. Analysis of the [RNQ+] prion reveals stability of amyloid fibers as the key determinant of yeast prion variant propagation. J Biol Chem 2010;285:20748–55.
[77] King CY, Wang HL, Chang HY. Transformation of yeast by infectious prion particles. Methods 2006;39:68–71.
[78] Cox B, Ness F, Tuite M. Analysis of the generation and segregation of propagons: entities that propagate the [PSI+] prion in yeast. Genetics 2003;165:23–33.
[79] Saibil HR, Seybert A, Habermann A, Winkler J, Eltsov M, Perkovic M, et al. Heritable yeast prions have a highly organized three-dimensional architecture with interfiber structures. Proc Natl Acad Sci USA 2012;109:14906–11.
[80] Kryndushkin DS, Engel A, Edskes H, Wickner RB. Molecular chaperone Hsp104 can promote yeast prion generation. Genetics 2011;188:339–48.
[81] Morales R, Duran-Aniotz C, Castilla J, Estrada LD, Soto C. De novo induction of amyloid-beta deposition in vivo. Mol Psychiatry 2012;17:1347–53.
[82] Chernoff YO, Derkach IL, Inge-Vechtomov SG. Multicopy SUP35 gene induces de-novo appearance of psi-like factors in the yeast *Saccharomyces cerevisiae*. Curr Genet 1993;24:268–70.
[83] Sherman F, Fink GR, Hicks JB. Methods in yeast genetics. In: Sherman F, Fink GR, Hicks JB, editors. Methods in Yeast Genetics. Plainview, New York: Cold Spring Harbor Lab; 1986.
[84] Serio TR, Cashikar AG, Moslehi JJ, Kowal AS, Lindquist SL. Yeast prion [psi +] and its determinant, Sup35p. Methods Enzymol 1999;309:649–73.
[85] Clos J, Brandau S. pJC20 and pJC40—two high-copy-number vectors for T7 RNA polymerase-dependent expression of recombinant genes in *Escherichia coli*. Protein Expr Purif 1994;5:133–7.
[86] Derkatch IL, Bradley ME, Liebman SW. Overexpression of the SUP45 gene encoding a Sup35p-binding protein inhibits the induction of the de novo appearance of the [PSI+] prion. Proc Natl Acad Sci USA 1998;95:2400–5.
[87] Tanaka M, Weissman JS. An efficient protein transformation protocol for introducing prions into yeast. Methods Enzymol 2006;412:185–200.
[88] Tuite MF, Mundy CR, Cox BS. Agents that cause a high frequency of genetic change from [psi$^+$] to [psi$^-$] in *Saccharomyces cerevisiae*. Genetics 1981;98:691–711.
[89] Bradley ME, Bagriantsev S, Vishveshwara N, Liebman SW. Guanidine reduces stop codon read-through caused by missense mutations in SUP35 or SUP45. Yeast 2003;20:625–32.
[90] Bagriantsev SN, Gracheva EO, Richmond JE, Liebman SW. Variant-specific [PSI+] infection is transmitted by Sup35 polymers within [PSI+] aggregates with heterogeneous protein composition. Mol Biol Cell 2008;19:2433–43.